Available online at www.sciencedirect.com
ScienceDirect
Virology 357 (2007) 215–227
VIROLOGY
www.elsevier.com/locate/yviro

Coronavirus nucleocapsid protein is an RNA chaperone

Sonia Zúñiga [a], Isabel Sola [a], Jose L. Moreno [a], Patricia Sabella [b], Juan Plana-Durán [b], Luis Enjuanes [a,*]

[a] *Centro Nacional de Biotecnología, CSIC, Department of Molecular and Cell Biology, Campus Universidad Autónoma, Darwin 3, Cantoblanco, 28049 Madrid, Spain*
[b] *Fort-Dodge Veterinaria, Department of Research and Development, Girona, Spain*

Received 29 June 2006; returned to author for revision 11 July 2006; accepted 29 July 2006
Available online 18 September 2006

Abstract

RNA chaperones are nonspecific nucleic acid binding proteins with long disordered regions that help RNA molecules to adopt its functional conformation. Coronavirus nucleoproteins (N) are nonspecific RNA-binding proteins with long disordered regions. Therefore, we investigated whether transmissible gastroenteritis coronavirus (TGEV) N protein was an RNA chaperone. Purified N protein enhanced hammerhead ribozyme self-cleavage and nucleic acids annealing, which are properties that define RNA chaperones. In contrast, another RNA-binding protein, PTB, did not show these activities. N protein chaperone activity was blocked by specific monoclonal antibodies. Therefore, it was concluded that TGEV N protein is an RNA chaperone. In addition, we have shown that purified severe acute respiratory syndrome (SARS)-CoV N protein also has RNA chaperone activity. *In silico* predictions of disordered domains showed a similar pattern for all coronavirus N proteins evaluated. Altogether, these data led us to suggest that all coronavirus N proteins might be RNA chaperones.

Keywords: RNA chaperone; Coronavirus; Nidovirus; RNA synthesis

Introduction

RNA molecules easily misfold because of their structural and functional flexibility and become trapped in inactive conformations that can be very stable and persistent (known as the RNA folding problem) (Herschlag, 1995). RNA chaperones are nucleic acid binding proteins, with broad specificity, that rescue RNAs trapped in unproductive folding states (Cristofari and Darlix, 2002; Herschlag, 1995; Lorsch, 2002; Schroeder et al., 2004). The main characteristic distinguishing RNA chaperones from other RNA-binding proteins is that, once the RNA has been folded, they are no longer needed and can be removed without altering RNA conformation. The number of proteins with RNA chaperone activity is growing steadily (Cristofari and Darlix, 2002; Rajkowitsch et al., 2005). There are several assays to analyze the RNA chaperone activity of a protein in vitro (Cristofari and Darlix, 2002), but only recently it has been shown that a protein acts as an RNA chaperone in vivo (Clodi et al., 1999; Mohr et al., 2002). This could be due, at least in part, to the pleiotropic effects that RNA chaperones can cause when they are mutated. In vitro, RNA chaperones (i) enhance ribozyme cleavage, (ii) enable rapid and accurate RNA annealing, and (iii) facilitate strand transfer and exchange. Among these activities, the first one is the most stringent for an RNA chaperone and requires the other two activities (Rajkowitsch et al., 2005).

There is a growing number of cellular RNA chaperones, both prokaryotic and eukaryotic (Cristofari and Darlix, 2002; Schroeder et al., 2004). However, up to date, only a few virus-encoded RNA chaperones have been described: (i) retroviral nucleocapsid proteins, the best studied being the NCp7 protein from human immunodeficiency virus (HIV-1) (Bertrand and Rossi, 1994; Hong et al., 2003; Tsuchihashi and Brown, 1994), (ii) delta antigen from hepatitis delta virus (HDV), that is the only protein encoded by this viroid RNA (Huang et al., 2003; Huang and Wu, 1998; Wang et al., 2003), (iii) the core protein from hepatitis C virus (HCV) (Cristofari et al., 2004), (iv) hantavirus N protein (Mir and Panganiban, 2005, 2006), and (v) poliovirus 3AB protein (DeStefano and Titilope, 2006). Most of these viruses have RNA genomes requiring tightly regulated

* Corresponding author. Fax: +34 91 585 4915.
E-mail address: L.Enjuanes@cnb.uam.es (L. Enjuanes).

0042-6822/$ - see front matter © 2006 Elsevier Inc. All rights reserved.
doi:10.1016/j.virol.2006.07.046

ribozyme activities, nucleic acid strand transfer, or annealing steps in their life cycle. Four of the virus-encoded RNA chaperones described (NCp7, HDV antigen, HCV core and Hantavirus N) are the nucleic acid binding proteins that pack the genomic RNA to form the viral ribonucleoproteins. These proteins are further required as RNA chaperones for several processes during replication and transcription.

The order *Nidovirales* includes enveloped single-stranded, positive-sense RNA viruses. A relevant characteristic of the members of this virus order is that the 5′ two-thirds of the entire RNA comprises open reading frames (ORFs) 1a and 1b encoding the replicase (*rep*) (Enjuanes et al., 2000b; Gorbalenya et al., 2006). *Nidovirales* comprise the *Coronaviridae* family that includes viruses with the largest known RNA genome, around 30 kb. The 3′ one-third of their genome includes the genes encoding the structural proteins, always in the order: 5′-S-E-M-N-3′ (Enjuanes et al., 2000a), and genes coding for non-structural proteins scattered among them. Coronaviruses have been classified in: (i) group 1, the most representative members being transmissible gastroenteritis virus (TGEV) and human coronavirus (HCoV)-229E, (ii) group 2a, the best studied being mouse hepatitis virus (MHV), (iii) group 2b, created after the discovery of the agent causing the severe acute respiratory syndrome (SARS), and (iii) group 3, the most representative member being the infectious bronchitis virus (IBV) (Enjuanes et al., 2000a; Gorbalenya et al., 2006). The study of the molecular biology of coronaviruses has increased its relevance since the identification of SARS-CoV (Drosten et al., 2003; Fouchier et al., 2003; Holmes and Enjuanes, 2003; Ksiazek et al., 2003; Kuiken et al., 2003; Marra et al., 2003; Rota et al., 2003) and the discovery of new human coronaviruses such as NL63 and HKU1 (van der Hoek et al., 2004; Woo et al., 2005). Infectious cDNA clones and replicons have been engineered by our group for TGEV (Almazan et al., 2004; Almazán et al., 2000; González et al., 2002) and SARS-CoV (Almazan et al., 2006), although other infectious clones are available for several coronaviruses (St-Jean et al., 2006; Thiel et al., 2001; Youn et al., 2005; Yount et al., 2000, 2003).

Coronavirus replication and transcription are based on RNA-dependent RNA synthesis. Replication of coronaviruses results in a full-length copy of the genomic RNA (gRNA), whereas transcription leads to the generation of a nested set of subgenomic mRNAs of various sizes (Pasternak et al., 2006). These mRNAs are 5′ and 3′-coterminal with the genome. A leader sequence of 65 to 93 nucleotides, derived from the 5′ end of the genome, is fused to the 5′ end of the mRNA coding sequence (body) by a discontinuous transcription mechanism (Pasternak et al., 2001; Sawicki and Sawicki, 1998; Zuñiga et al., 2004). This process resembles a high-frequency similarity-assisted copy-choice RNA recombination (Brian and Spaan, 1997; Nagy and Simon, 1997; Pasternak et al., 2003), in which the transcription regulating sequences (TRSs) of the body (TRS-B, donor) and leader (TRS-L, acceptor), located in distal domains in the RNA primary structure, are probably brought into physical proximity by RNA–protein and protein–protein interactions. In fact, members of the heterogeneous nuclear ribonucleoprotein (hnRNP) family, like hnRNP A1 and the polypyrimidine tract binding protein (PTB), are involved in MHV RNA synthesis (Choi et al., 2002; Huang and Lai, 2001; Shi et al., 2000).

Coronavirus nucleocapsid (N) protein has a structural role as it forms a ribonucleoprotein complex with gRNA. N protein probably also has an important role in RNA synthesis (Baric et al., 1988; Laude and Masters, 1995). In fact, at early times postinfection, it colocalizes with the replication complex in the sites of RNA synthesis (Bost et al., 2001; Denison et al., 1999), and only background levels of coronavirus RNA synthesis are produced in the absence of N protein (Almazan et al., 2004; Schelle et al., 2005). Although nucleoproteins from different coronaviruses are variable in length and primary sequence, a conserved three-domain organization was proposed (Parker and Masters, 1990). N protein domain II is more conserved than domains I and III, especially in a serine-rich region that is probably important for the biological function of N protein. Recently, a modular organization without correlation with the previously proposed three-domain structure, based on protein disorder and common for all coronavirus N proteins, has been proposed (Chang et al., 2006). Several domains in the N protein have been mapped, such as the RNA-binding (Fan et al., 2005; Huang et al., 2004; Nelson et al., 2000) and the oligomerization (Fan et al., 2005; Hurst et al., 2005; Yu et al., 2005) domains.

In this report, we show that the N proteins from two coronaviruses (TGEV and SARS-CoV) have RNA chaperone activity. The possible conservation of this activity in coronavirus N proteins and its potential role in RNA synthesis is discussed.

Results

Coronavirus N protein as an RNA chaperone candidate

Coronavirus N protein packs the genomic RNA, as do the previously described virus-encoded RNA chaperones (Cristofari et al., 2004; Huang and Wu, 1998; Levin et al., 2005). RNA chaperones possess the highest frequency of intrinsically disordered regions (Ivanyi-Nagy et al., 2005; Tompa and Csermely, 2004). A modular organization of coronavirus N protein has been proposed using the PONDR VSL1 predictor (Iakoucheva et al., 2002; Romero et al., 1997), with two organized domains separated by unstructured regions (Chang et al., 2006). Intrinsically disordered regions of several coronavirus N proteins were postulated using the DisProt VL3H predictor (Obradovic et al., 2003; Peng et al., 2005), previously used for the analysis of the correlation between intrinsic disorder and chaperone function (Ivanyi-Nagy et al., 2005) (Fig. 1). RNA-binding (Fan et al., 2005; Huang et al., 2004; Nelson et al., 2000) and oligomerization (Fan et al., 2005; Hurst et al., 2005; Yu et al., 2005) domains previously characterized have been included in the graphic representations (Fig. 1, hatched regions). A good correlation between the presence of disordered and ordered regions and the 3D structure of different domains has been identified (Fan et al., 2005; Huang et al., 2004), validating *in silico* predictions of N protein domains. Long disordered regions were predicted in all the N proteins analyzed (Fig. 1), postulating

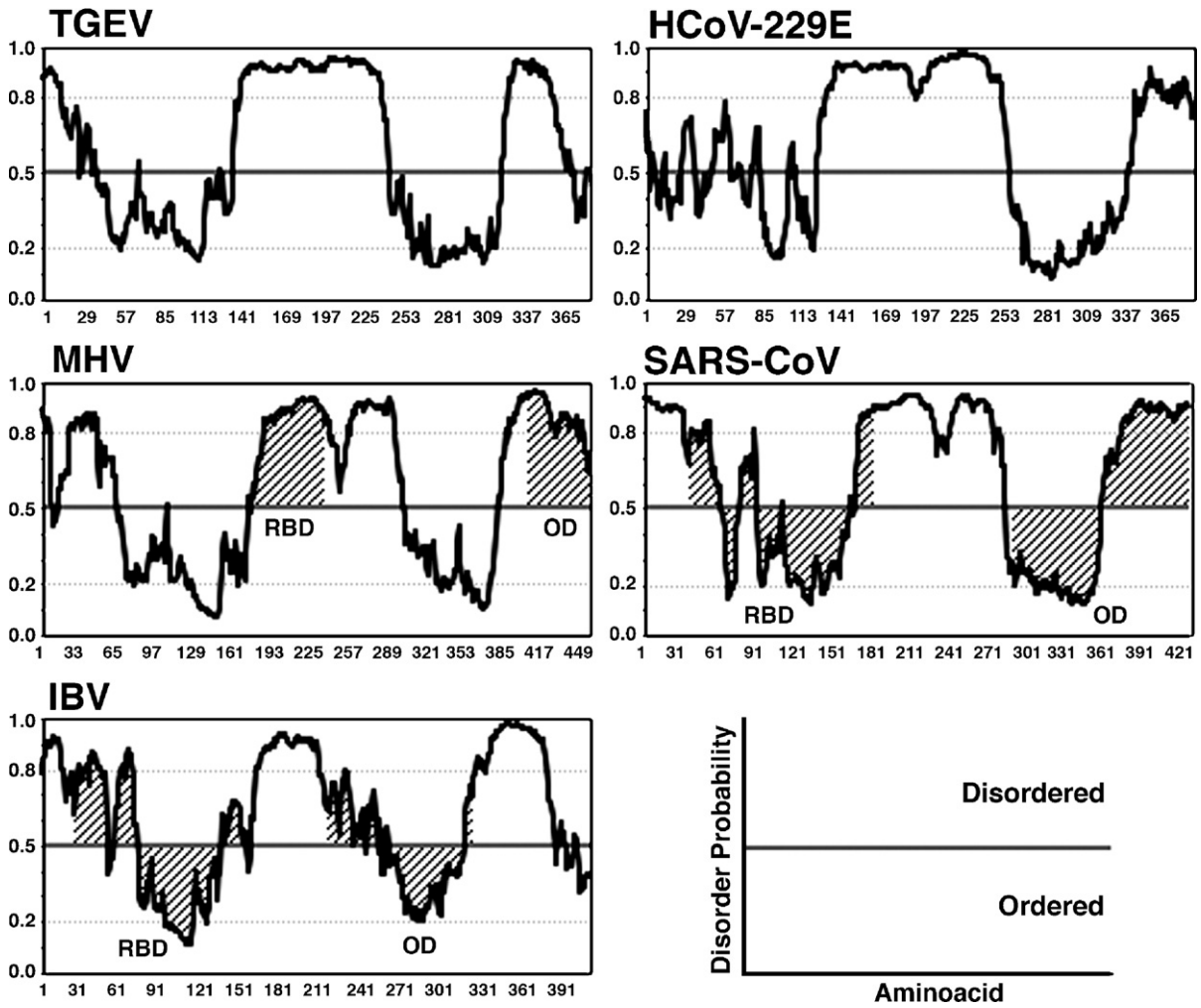

Fig. 1. Prediction of intrinsically unstructured regions in coronavirus N proteins. Graphical representation of the disorder probability vs. amino acid position of N proteins determined using DisProt VL3H. Nucleoproteins from coronavirus group 1 (TGEV, HCoV-229E), group 2a (MHV), group 2b (SARS-CoV), and group 3 (IBV) were analyzed. As indicated in the lower panel on the right, amino acids with a disorder score equal or above 0.5 are considered to be in a disordered environment, while a value below 0.5 is considered ordered. The percentage of disorder covers more than 50% of the sequence in all cases: 52.62% (TGEV), 57.53% (HCoV-229E), 57.27% (MHV), 61.85% (SARS-CoV), and 62.35% (IBV). Hatched regions indicate previously identified RNA-binding (RBD) and oligomerization (OD) domains.

that more than 50% of their residues were in unstructured regions, as expected for nucleic acid chaperones (Ivanyi-Nagy et al., 2005). These observations, and the capacity of N protein to bind RNA nonspecifically, opened the possibility that N protein was an RNA chaperone candidate.

Recombinant N protein binds RNA nonspecifically

Previous results have shown that coronavirus N protein binds RNA nonspecifically, although a higher affinity for leader and TRSs sequences was described (Nelson et al., 2000). In addition, in a recent report, it has been shown that IBV phosphorylated N protein has higher affinity for viral sequences, especially leader TRS, than for random RNAs (Chen et al., 2005). As a previous step to analyze the RNA chaperone activity of N protein, its binding to RNA was tested. TGEV nucleoprotein was expressed in *Escherichia coli* and purified as a GST-tagged protein. The purified N protein was incubated with an excess of different RNA oligonucleotides, representing viral TRSs or a cellular RNA, and the binding of N protein to RNA was detected by electrophoretic mobility shift assay (EMSA). A band shift was observed in all cases (Fig. 2A), indicating that GST-N protein bound RNA with broad specificity, as expected.

Blocking of TGEV N protein–RNA binding

A set of monoclonal antibodies (mAbs) recognizing different domains of TGEV N protein, produced in our laboratory (Martín-Alonso et al., 1992), was used to analyze their effect in TRS-L binding (Fig. 2B). The objective of this study was to select some antibodies for the subsequent analyses of N protein RNA chaperone activity. EMSA studies showed that mAbs recognizing the amino terminus domain of the protein (1–241aa) significantly interfered with RNA binding, inhibiting band shift (Fig. 2C), whereas mAbs specific for the carboxy terminus did not hamper protein–RNA binding leading to a supershift band in all cases. These bands probably correspond to complex molecular aggregates of high molecular

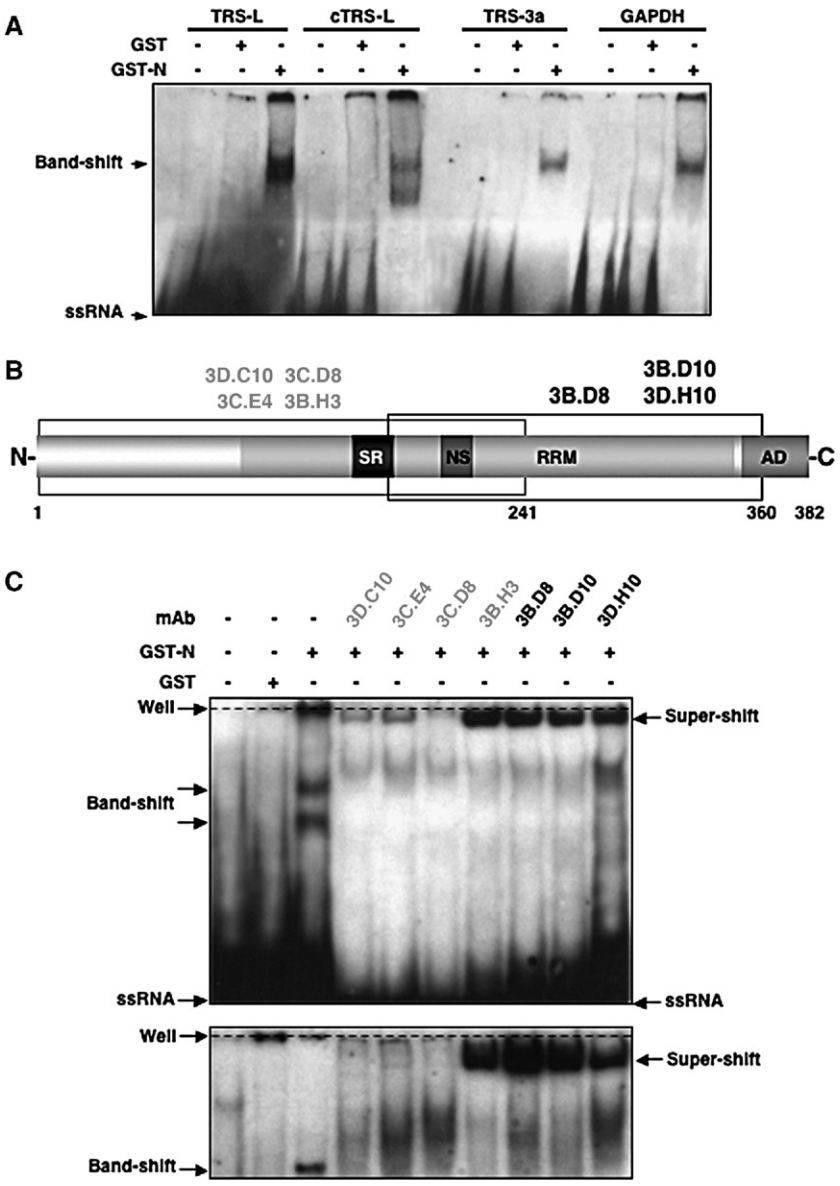

Fig. 2. TRS-binding domain in TGEV N protein. (A) EMSA result after incubation of 300 ng of negative control, GST or GST-N proteins with 10 pmol of 5′-biotinylated RNA oligonucleotides (Table 1). TRS, transcription-regulating sequence; cTRS, sequence complementary to the TRS; GST, glutathione *S*-transferase; GAPDH, glyceraldehyde-3-phosphate dehydrogenase; ssRNA, single-stranded RNA. (B) Scheme of N protein domains and epitopes recognized by mAbs. Numbers under the scheme indicate amino acid positions in the protein. SR, serine-rich domain; NS, nuclear localization signal; AD, acidic domain; RRM, RNA-recognition motif. (C) EMSA result after incubation of 300 ng of protein and 1 pmol of TRS-L oligonucleotide. When indicated, on top of the lanes, recombinant N protein was preincubated with the indicated mAb. The apparent difference between the band shift found in this case and in the gel in A is probably due to the fact that in this case the electrophoresis was developed for a longer time in order to resolve the supershift complexes. Bottom, fragment of the EMSA result after longer electrophoresis time, allowing the supershift complexes to enter the gel.

weight that clearly moved into the gel, although only migrated a short distance. mAb 3B.H3, specific for the N-terminus of the protein, did not interfere with RNA binding as it likely binds to a different epitope than mAbs 3D.C10, 3C.E4, and 3C.D8. A weak and diffuse band, migrating between the shifted and supershifted bands, appeared only in the lanes including mAbs. The presence of this band was probably due to minor RNA–protein complexes formed between the viral RNA and proteins present in the hybridoma supernatants used as the source of mAbs as it is absent when hybridoma supernatants were not added to the EMSA reactions (Fig. 2C, lanes 1 to 3). These results suggested that the RNA-binding domain is likely located at the amino terminus half of the N protein, in agreement with previously described RNA-binding domains of MHV, SARS-CoV, and IBV (Fan et al., 2005; Huang et al., 2004; Nelson et al., 2000). Additional experiments are needed to precisely determine the exact RNA-binding motif of the protein.

Enhancement of avocado sunblotch viroid (ASBVd) ribozyme self-cleavage by TGEV N protein

To analyze whether N protein acts in vitro as an RNA chaperone, an advanced assay was used. ASBVd is a plant viroid that requires a hammerhead-mediated self-cleavage of

oligomeric ASBVd RNA during its replication following the rolling circle mechanism (Daròs et al., 1994). One of the most representative properties of nucleic acid chaperones is the ability of these proteins to enhance hammerhead ribozyme activity (Daros and Flores, 2002).

ASBVd positive-sense dimeric RNA was in vitro transcribed and biotin labeled. The predicted secondary structure for this RNA contains most of the nucleotides in dsRNA regions, forming a rod-shaped structure with some stem-loops at one end. For ribozyme cleavage, an RNA reorganization to form two hammerhead ribozyme domains is required (Flores et al., 2000). ASBVd RNA was incubated, in cleavage conditions, in the absence or in the presence of recombinant GST or GST-N proteins. In the absence of protein, the transcript of 591 nt self-cleaved at 5 min yielding the expected products, especially the 247 nt completely cleaved RNA (Figs. 3A and B), although the self-cleavage reaction made no progress with incubation time. The same effect was observed by incubating the RNA with GST protein. In contrast, in the presence of GST-N protein, an enhancement of ribozyme self-cleavage was observed, suggesting that N protein had RNA chaperone activity. Other bands increased their intensity with the incubation time and also appeared in the absence of protein. These bands most likely resulted from RNA cleavage at sites particularly prone to nuclease attack (Daros and Flores, 2002). The increase in the appearance of these bands, and also of RNA degradation, was probably due to the RNA chaperone activity of N protein that facilitates nuclease action (Levin et al., 2005). To exclude the possibility of co-purification of an *E. coli* RNA chaperone with GST-N protein and confirm that the increase in ribozyme cleavage was due to TGEV N protein, the recombinant protein was incubated with purified mAbs 3D.C10 (blocking RNA binding) and 3B.D10 (that did not block this binding). Monoclonal antibody 3D.C10 significantly inhibited the ribozyme cleavage enhancement produced by the GST-N

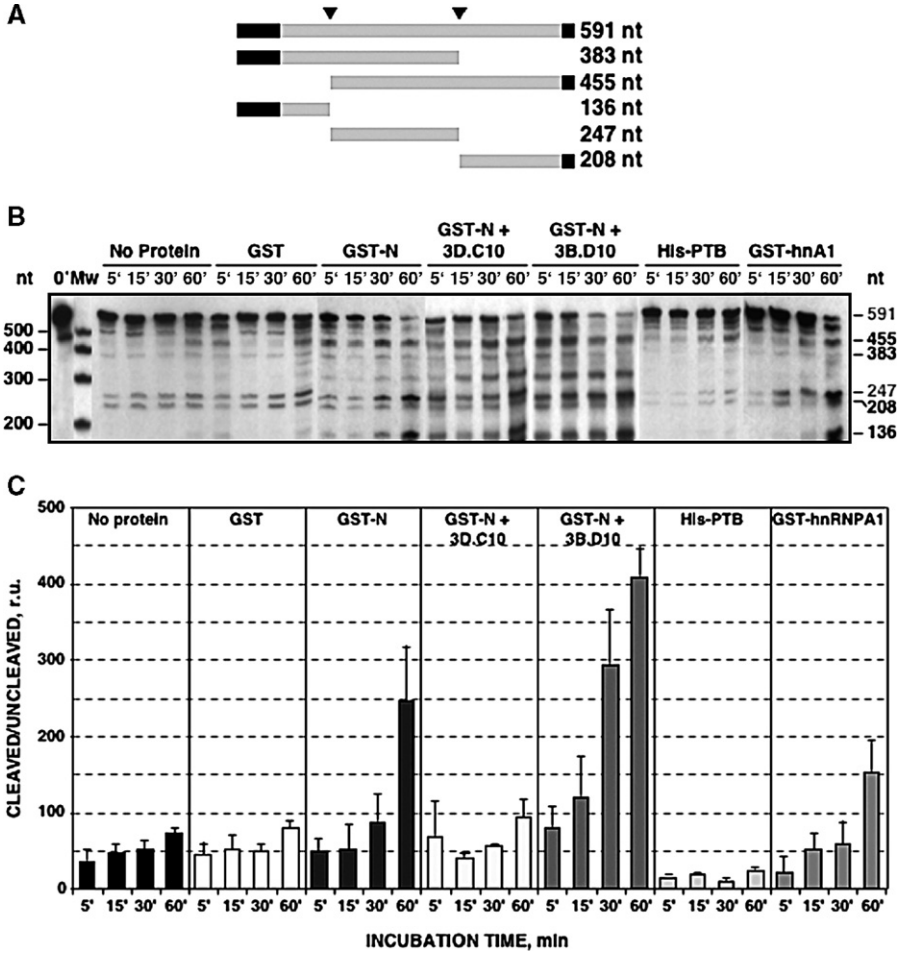

Fig. 3. Recombinant TGEV N protein enhances ribozyme self-cleavage. (A) Scheme of the ASBVd in vitro transcript with ribozyme cleavage sites indicated by arrowheads. Vector and viroid sequences are represented by black and gray bars, respectively. All products resulting from ribozyme self-cleavage are indicated. Numbers on the right of the figure indicate the size, in nucleotides, of each RNA product. (B) Time-course of ribozyme self-cleavage reaction. Biotinylated RNA (25 ng) was incubated in the absence or presence of 300 ng of protein, and reaction mixture aliquots were collected and frozen at indicated time points. On top of each lane, the reaction time (minutes) is indicated. Numbers on the left of the panel indicate the size markers (Mw) in nucleotides. Numbers on the right of the panel indicate the cleavage products size. Uncleaved (591 nt) and completely cleaved (247 nt) products are marked in gray. GST-hnA1, GST-hnRNPA1. (C) Densitometric quantification of ribozyme self-cleavage reactions. Bands corresponding to uncleaved (591 nt) and completely cleaved (247 nt) products were measured. After background correction, the ratio of cleaved to uncleaved product was calculated based on the division between these two intensities. Error bars indicate the standard deviation from three independent experiments.

protein while mAb 3B.D10 did not (Fig. 3B). As TGEV replicates in human cells (Almazan et al., 2004), two human cellular proteins were expressed and purified from *E. coli* and tested as controls: (i) hnRNP A1, a nucleic acid chaperone (Bertrand and Rossi, 1994; Herschlag et al., 1994; Portman and Dreyfuss, 1994), and (ii) PTB, an RNA-binding protein with no known RNA chaperone activity. To exclude that the effect of the N protein was simply due to its RNA-binding ability, the chaperone activity of recombinant His-PTB protein was evaluated. No enhancement of ribozyme self-cleavage was found with PTB protein (Fig. 3B), whereas recombinant GST-hnRNPA1 protein produced an increase in the ribozyme cleavage reaction similar to that observed with coronavirus N protein, as expected for an RNA chaperone (Fig. 3B).

Densitometry of the RNA fragments produced by the ribozyme self-cleavage from three independent experiments showed that the enhancement of self-cleavage produced by recombinant N protein was four-fold higher than in the absence of protein (Fig. 3C). This cleavage increase was comparable to that obtained in the presence of hnRNP A1 protein, a prototype RNA chaperone protein (Fig. 3C). Preincubation of N protein with mAb 3D.C10, to prevent N protein–RNA binding, reduced the ratio of cleaved to uncleaved substrate to the levels obtained in the absence of protein or in the presence of irrelevant proteins such as GST or His-PTB (Fig. 3C), confirming that the increment of ribozyme activity was specifically due to N protein. In addition, preincubation of N protein with mAb 3B.D10, that did not interfere with RNA–protein binding, enhanced the ribozyme cleavage up to six-fold compared with the cleaved to uncleaved ratio in the protein-free reactions (Fig. 3C). This result showed that the N protein with the carboxy terminus half blocked by the antibody was still active in the ribozyme enhancement. The higher cleavage efficiency observed in the presence of this mAb could be due to a change in the conformation of this protein that favors its chaperone activity or, alternatively, to the aggregation of the N protein caused by the mAb.

TGEV N protein promotes viral TRS annealing

The RNA chaperone activity of recombinant N protein in vitro was demonstrated with the ribozyme self-cleavage assay. Nevertheless, ASBVd is a heterologous system evolutionary distant from coronaviruses. Therefore, it was decided to determine the influence of TGEV N protein in RNA annealing reactions using coronavirus TRSs. Biotin-labeled TRS-L was hybridized with different amounts of unlabeled cTRS-7 as the annealing between TRS-L and cTRS-B is a crucial step in template switch during coronavirus transcription (Sola et al., 2005; Zuñiga et al., 2004). TRS-L oligonucleotide could generate species with different mobility (ssRNA′), apart from the single-stranded RNA (ssRNA) band indicated (Fig. 4A). TRS-L and cTRS-7 oligonucleotides annealed in vitro in the absence of protein. Nevertheless, TGEV N protein promoted their annealing (Fig. 4B). The increase in annealing promoted by N protein was noted even in the presence of magnesium (data not shown) that stabilized double-stranded RNAs (dsRNAs). In the reaction conditions, there was no change in the amount of ssRNA′ species. As the incubations were performed for 30 min, it is possible that this band could disappear with longer incubation times. At this moment, there are no available data indicating whether the ssRNA′ species are unproductive TRS-L conformations or whether they are intermediate products that accumulate in the generation of the dsRNA. The increased annealing was reproduced in three experiments, and the ratio of dsRNA to ssRNA was quantified after resolving these RNAs in a gel. Recombinant N protein significantly increased the ratio of dsRNA to ssRNA (Fig. 4C). This effect was due to N protein and not to molecular crowding as GST protein alone, used in the same molar amount, did not exert any influence on TRSs annealing (Figs. 4B and C). Specific binding of PTB to viral TRSs (Zuñiga S., Sola I., Moreno J.L. and Enjuanes L., unpublished results) did not promote TRSs annealing reaction (Figs. 4B and C), confirming the TGEV N protein RNA chaperone activity in the context of coronavirus TRSs.

TGEV N protein promotes DNA oligonucleotide annealing

RNA chaperones promote nucleic acids annealing and also unwinding. Therefore, the final ratio of double to single-stranded nucleic acid detected is the result of both activities. The nature of the oligonucleotides used in the assay and the ionic strength of the solution also influence annealing reactions (Levin et al., 2005). Therefore, to reinforce the conclusions obtained from the annealing of viral RNAs, similar reactions were performed using previously described DNA oligonucleotides (Huang et al., 2003) (Fig. 5A), expecting that, as an RNA chaperone, TGEV N protein could also promote DNA annealing. In the presence of recombinant N protein, the level of dsDNA was significantly higher than in its absence or in the presence of control proteins, such as GST and PTB. The annealing promoted by N protein was similar to that obtained in the presence of a reference RNA chaperone such as hnRNP A1 (Fig. 5B). Furthermore, after annealing reactions, proteinase K was added to eliminate the protein from the reaction mixture, and the amount of dsDNA did not significantly decrease after annealing promotion by N or hnRNP A1 (Fig. 5B), as expected for RNA chaperones. These data confirmed that TGEV N protein behaves as a nucleic acid chaperone.

RNA chaperone activity of SARS-CoV N protein

Despite the poor conservation of coronavirus N protein sequences, regions with functional relevance are highly conserved. Predicted secondary structure and disordered regions of coronavirus N proteins are also conserved (Calvo et al., 2005) (Fig. 1). To investigate whether RNA chaperone activity was present in other coronavirus N proteins, SARS-CoV N protein was selected as it is relatively distant from TGEV N protein with only 34% amino acid identity between them. The self-cleavage of biotin-labeled ASBVd dimeric RNA was monitored in the absence or in the presence of SARS-CoV N-His protein expressed by a recombinant baculovirus and purified from

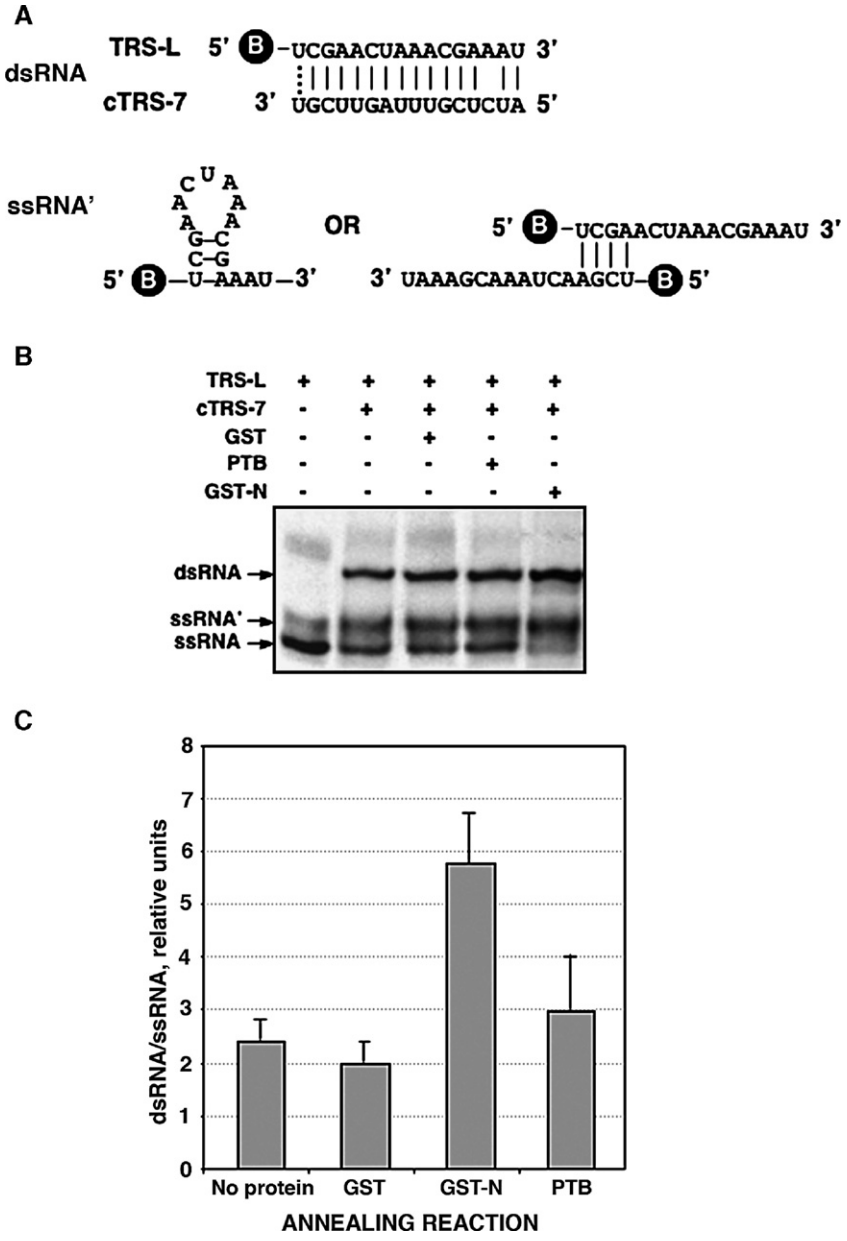

Fig. 4. Recombinant TGEV N protein promotes viral TRSs annealing. (A) Scheme of the duplex formed by viral TRS-L and cTRS-7 and the possible structures formed by TRS-L. (B) Annealing reactions in the absence or presence of 300 ng of recombinant protein. Biotin-labeled TRS-L 0.025 μM was incubated with 0.025 μM of unlabeled cTRS-7. PTB, His-PTB. (C) Annealing of TRS-L and cTRS-7 was repeated three times, and the bands indicated as dsRNA and ssRNA were quantified. Ratio of dsRNA to ssRNA is presented for each case. Error bars indicate the standard deviation.

insect cells. Recombinant N-His protein enhanced ribozyme self-cleavage (Fig. 6A), indicating that this protein has RNA chaperone activity. RNA degradation was stronger in these reactions compared with that obtained in the presence of TGEV N protein. This increase could be due to a higher chaperone activity of the N-His protein, leading to an increased nuclease activity. Densitometry of the RNAs from three independent experiments showed that N-His protein enhanced ribozyme cleavage up to ten-fold compared with the protein free reactions (Fig. 6B). The higher enhancement efficiency of SARS-CoV N protein, in relation to that of TGEV N protein, was possibly due to a more native conformation of SARS-CoV N protein as a consequence of the presence of a smaller tag, distant from RNA-binding domain, located in the carboxy terminus, or to the expression of this protein in insect cells, leading to a protein with post-translational modifications such as phosphorylation.

Discussion

The RNA chaperone activity of two coronavirus N proteins is described, representing the first report of a coronavirus protein with RNA chaperone activity. N protein has a structural role in coronavirus assembly (Risco et al., 1996), and there is a growing evidence for a role of this protein in RNA synthesis (Almazan et al., 2004; Baric et al., 1988; Nelson et al., 2000; Schelle et al., 2005; Stohlman et al., 1988). In addition, N

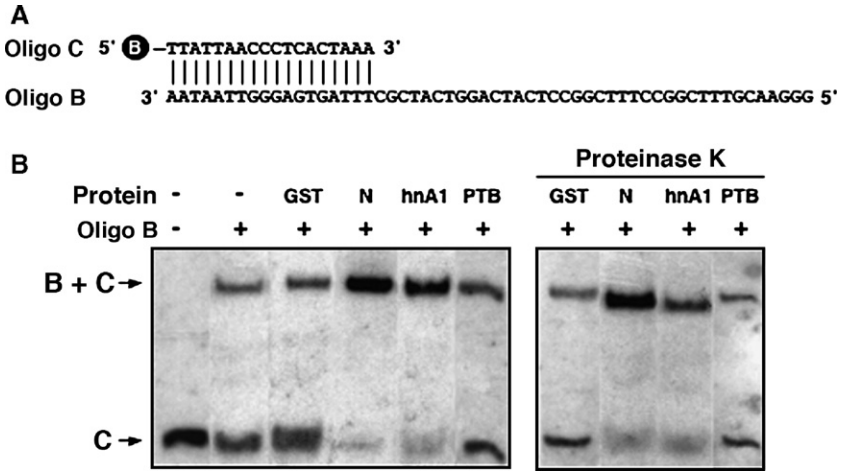

Fig. 5. Recombinant TGEV N protein promotes DNA oligonucleotides annealing. (A) Scheme of the duplex formed by DNA oligonucleotides C and B (Huang et al., 2003). (B) Annealing reactions in the absence or presence of 300 ng of recombinant protein. Biotin-labeled oligo C 0.5 nM was incubated with 0.4 nM of unlabeled oligo B. The bands corresponding to dsDNA (B+C) and ssDNA (C) are indicated. After the annealing reaction was completed, proteinase K (150 μg/ml) was added to eliminate the protein when indicated. N, GST-N; hnA1, GST-hnRNP A1; PTB, His-PTB.

protein displays pleiotropic effects when expressed in the cell, such as induction of apoptosis or cell-cycle arrest (He et al., 2003; Surjit et al., 2004). The relevance of N protein in coronavirus RNA synthesis, its nonspecific binding to RNA and its intrinsic disorder led us to investigate N protein potential nucleic acid chaperone activity. It was found that, at least in vitro, TGEV N protein had RNA chaperone activity, enhancing ASBVd hammerhead ribozyme self-cleavage as typical RNA chaperones do (Daros and Flores, 2002). These results imply that N protein promotes the correct folding of the hammerhead ribozyme avoiding unproductive RNA conformations, therefore acting as an RNA chaperone. Interestingly, it was found that N protein also promotes annealing in vitro of DNA and viral TRS RNAs, confirming its role as an RNA chaperone in a coronavirus-related system.

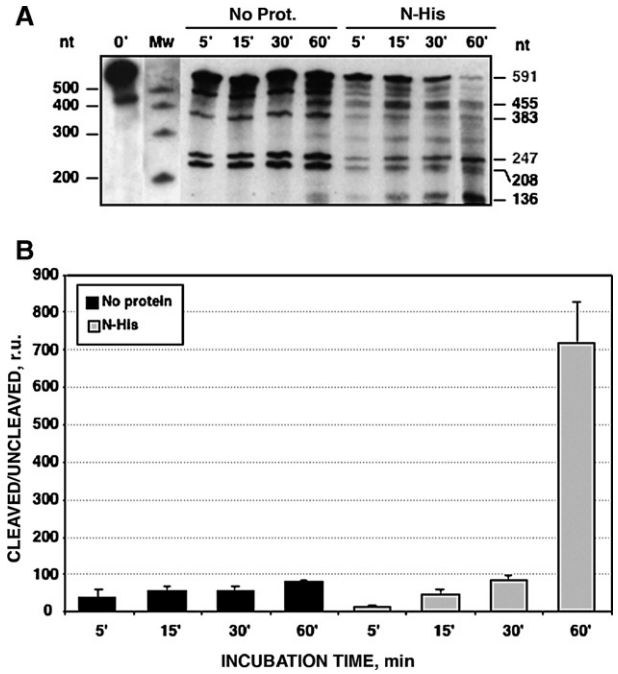

Fig. 6. Enhancement of ribozyme self-cleavage by recombinant SARS-CoV N protein. (A) Time-course of ASBVd ribozyme self-cleavage reaction, performed as previously described (see above). On top of each lane, reaction time (minutes) is indicated. Numbers on the left of the panel indicate the molecular mass (Mw) in nucleotides. Numbers on the right of the panel indicate the cleavage products in nucleotides. Uncleaved (591 nt) and completely cleaved (247 nt) products are marked in gray. Note that the gel corresponding to the reaction in the absence of protein is over-exposed to detect cleavage products and smaller bands. (B) Densitometric quantification of ribozyme self-cleavage reactions. Error bars indicate the standard deviation from three independent experiments.

TGEV N protein binding domain for TRS RNA is likely located within the first 241 aa of this protein as mAbs specific for this region significantly inhibited RNA-N binding. This result agrees with previous data locating MHV N leader-binding domain between aa 177 and 231, a region including the Ser-rich motif conserved in all coronavirus N proteins (Nelson et al., 2000).

N protein primary sequence is not highly conserved among coronaviruses from different groups, although some sequence motifs with functional relevance are highly conserved. The predicted secondary structure of N proteins is also conserved (Calvo et al., 2005). It was recently described that RNA chaperones are the protein class with the highest frequency of long intrinsically disordered regions. These domains frequently have high functional relevance, and an entropy transfer model for chaperone function has been proposed (Tompa and Csermely, 2004). According to this model, binding of an RNA chaperone to the substrate (RNA) is accompanied by local folding of the previously disordered regions of the protein, with a concomitant unfolding of an RNA region. After several cycles of disorder-to-order and order-to-disorder transitions, the final result is that the RNA is folded in the proper conformation and released to form the RNA chaperone (Tompa and Csermely, 2004). Prediction of disordered regions in N proteins from several coronaviruses showed that there is a great conservation in the length, position, and frequency of these regions. In addition, our experimental data indicated that SARS-CoV N protein has also RNA chaperone activity. All these observations

led us to postulate that RNA chaperone activity is not an exclusive characteristic of TGEV N protein, but might be a general activity of all coronavirus nucleoproteins.

The phosphorylation of TGEV N protein has been recently reported (Calvo et al., 2005). A comparable post-translational modification has also been described for IBV N protein (Chen et al., 2005). The role of phosphorylation is still unclear, although it was proposed that phosphorylated IBV N protein preferentially binds viral than cellular RNAs (Chen et al., 2005). It is worth noting that the recombinant TGEV N protein used in this study was not post-translationally modified as it was expressed in *E. coli*. Nevertheless, this N protein bound viral TRSs and had RNA chaperone activity, indicating that phosphorylation is not essential for N protein chaperone activity. On the other hand, SARS-CoV N-His protein showed higher activity than TGEV N protein. SARS-CoV N-His protein was expressed using a baculovirus system, allowing post-translational modifications. Therefore, it is tempted to speculate that perhaps a post-translational modification, such as N protein phosphorylation, could increase its RNA chaperone activity or have a role in RNA-binding affinity.

Due to the large size of coronavirus RNA genome and the template switch required during transcription, coronavirus RNA synthesis may require the assistance of RNA chaperones. Recent data showed that the free energy of the duplex formation between cTRS-B and TRS-L is probably the main factor, although not the only one, in coronavirus discontinuous transcription (Sola et al., 2005; Zuñiga et al., 2004). An energy barrier must be overcome to dissociate the nascent minus RNA chain from the genomic template and to perform a template switch with the TRS of the leader. RNA chaperones are proteins that could decrease this energy threshold.

Other cellular RNA chaperones may also exert in vivo an effect on coronavirus RNA synthesis. In fact, the hnRNP A1 protein, binding coronavirus RNA (Huang and Lai, 2001; Shi et al., 2000), is an RNA chaperone (Bertrand and Rossi, 1994; Pontius and Berg, 1992; Portman and Dreyfuss, 1994). Nevertheless, previous data on coronavirus RNA synthesis (Almazan et al., 2004; Schelle et al., 2005) generated in the presence of cellular chaperones and in the absence of N protein indicate that N protein has an important role in coronavirus RNA synthesis. To our knowledge, the activity of a virus-encoded RNA chaperone in vivo using a mammalian system has not been described as the in vivo data reported up to date have been generated using a bacterial RNA folding trap (Clodi et al., 1999). Work in progress in our laboratory is focused to determine the role of the N protein in vivo as an RNA chaperone in coronavirus transcription, especially in template switch, taking advantage of the reverse genetics tools available.

Materials and methods

Plasmid constructs

TGEV N gene, nucleotides 26,917 to 28,065 from the genome (GeneBank accession number AJ271965), was amplified by PCR using the TGEV infectious cDNA as template (Almazán et al., 2000), oligonucleotides N1 (5′-ATGGCCAACCAGGGACAACGTG-3′) and N1148 (5′-TTAGTTCGTTACCTCATCAATTATC-3′) and Platinum *Pfx* polymerase (Invitrogen) according to manufacturer's instructions. The 1149 bp PCR product was cloned on pGEX-4T-2 vector (Amersham Biosciences) digested with *Sma*I. The resulting pGEX4T2-N plasmid directed the expression of a recombinant GST-N fusion protein.

SARS-CoV Urbani strain N gene, nucleotides 28,120 to 29,388 from the genome (GeneBank accession number AY278741), was amplified by PCR using as template the SARS-CoV cDNA clone (Almazan et al., 2006), oligonucleotides SARS-N-VS (5′-CACGGAATTCATGTCTGATAATGGACCCCAATC-3′) and SARS-N-RS (5′-GTACGCTCGAGTGCCTGAGTTGAATCAGCAGAAG-3′) and Platinum *Pfx* polymerase (Invitrogen) according to manufacturer's instructions. The 1286 bp PCR product was digested with *Eco*RI and *Xho*I restriction enzymes and cloned in the donor plasmid pFastBAC-Cter-HisTag, a generous gift from A. Alcamí (CNB, CSIC). The resulting pFastBac-N-SARS-Cter-HisTag was the donor plasmid for the expression of a recombinant N-His fusion protein.

Human hnRNP A1 isoform A was cloned from plasmid pET9d-hnRNPA1, kindly provided by A. Krainer (Cold Spring Harbor Laboratory). The gene was amplified by PCR using oligonucleotides hnRNPA1-VS (5′-CGGGATCCATGTCTAAGTCAGAGTCTCC-3′) and hnRNPA1-RS (5′-CCGAATTCTTAAAATCTTCTGCCACTGC-3′) and Platinum *Pfx* polymerase (Invitrogen) according to manufacturer's instructions. The 1119 bp PCR product was digested with *Bam*HI and *Eco*RI restriction enzymes and cloned in the same sites of pGEXT-4T-2. The resulting pGEX4T2-hnRNPA1 plasmid directed the expression of a recombinant GST-hnRNPA1 fusion protein.

All cloning steps were checked by sequencing the PCR amplified fragments, fusion genes, and cloning junctions.

Plasmids pET28a-PTB (Xie et al., 2003) and pBdASBVd [A28] (Daros and Flores, 2002) were generous gifts from D. Black (Howard Hughes Medical Institute, UCLA) and J.A. Daròs (Plant Molecular and Cell Biology Institute, UPV), respectively.

Recombinant baculovirus expressing SARS-CoV N protein

Bac-to-Bac Baculovirus Expression System (Invitrogen) was used following manufacturer's instructions. Briefly, the recombinant baculovirus genome was obtained by electroporation of *E. coli* DH10Bac cells (Invitrogen) as described (Airenne et al., 2003). To obtain the recombinant baculovirus, High Five insect cells were transfected using Cellfectin reagent (Invitrogen) following manufacturer's specifications. Cytopathic effect was observed at 72 h post-transfection, and the supernatant containing the recombinant baculovirus was harvested at 5 days post-transfection.

Protein expression and purification

E. coli cells of the strain BL21(DE3)pLys (Novagen) were transformed with plasmids pGEX-4T-2, pGEX4T2-N,

pGEX4T2-hnRNPA1, or pET28a-PTB. For GST, GST-N and GST-hnRNPA1 expression and purification, a 250 ml culture was grown at 37 °C to approximately 0.5 OD_{600}. Protein expression was induced with 1 mM ITPG for 4 h at 30 °C. The cell pellet was resuspended in CelLytic B II (Sigma) with Protease Inhibitor Cocktail (Sigma), and protein extract was obtained following manufacturer's instructions. From this extract, recombinant proteins were purified using glutathione Sepharose 4B (Amersham Biosciences) according to manufacturer's specifications. His-PTB protein was purified as previously described (Xie et al., 2003), using the same bacterial lysis protocol and HIS-Select Nickel affinity gel (Sigma) following manufacturer's instructions. To purify SARS-CoV N-His protein, High Five insect cells were grown on 150 mm plates and infected with the recombinant baculovirus. At 48 hpi, the cells were harvested and resuspended in lysis buffer (50 mM sodium phosphate buffer pH 8.0, 300 mM NaCl, 0.05% Tween-20, and 1% NP-40) with Protease Inhibitor Cocktail (Sigma). The protein extract was recovered after 10 min incubation on ice and 10 min centrifugation 10,000×*g* at 4 °C. Recombinant N-His protein was purified from this extract using HIS-Select Nickel affinity gel (Sigma) following manufacturer's instructions.

All the purification steps were followed by Coomassie staining, using EZBlue (Sigma), and by Western blot analysis with specific antibodies. To detect GST-N and N-His proteins, mAbs 3D.H10 (Martín-Alonso et al., 1992) and anti-polyhistidine peroxidase conjugated antibody (Sigma) were used, respectively. Recombinant GST-hnRNPA1 protein was detected using polyclonal antibody E-17 (Santa Cruz Biotechnology). Hybridoma cells BB7, producing mAb against human PTB, used for His-PTB detection, were purchased from ATCC.

RNAs

5′ biotinylated or unmodified RNA oligonucleotides, described in Table 1, were purchased form CureVac (Tübingen, Germany). Biotin-labeled dimeric ASBVd (+) RNA was synthesized by in vitro transcription of *Xba*I linearized pBdASBVd[A28] template, using MEGAscript T7 kit (Ambion) and biotin-14-CTP (Invitrogen), following manufacturer's instructions. The transcript was purified by 2% low-melting agarose gel electrophoresis. After electrophoresis, the band corresponding to the non-cleaved biotinylated RNA was cut and melted at 60 °C. The RNA was cleaned using the RNeasy Mini kit (Qiagen), according to manufacturer's specifications and eluted in 1 mM EDTA pH 8.0.

IgGs purification

mAbs 3D.C10 and 3B.D10 (Martín-Alonso et al., 1992) were isolated from hybridoma culture supernatants using the Protein A Antibody Purification Kit (Sigma) according to manufacturer's instructions. To minimize nuclease contamination during the assays, these purified antibodies were used in the presence of a broad range nuclease inhibitor (SUPERase●In, Ambion).

Table 1
RNA oligonucleotides

Name	Oligonucleotide sequence 5′→3′ [a]	Position in TGEV genome
TRS-L	Bio-UCGAACUAAACGAAAU	89–104
cTRS-L	Bio-AUUUCGUUUAGUUCGA	104–89
TRS-3a	Bio-AAGAACUAAACUUACG	24,793–24,808
cTRS-3a	Bio-CGUAAGUUUAGUUCUU	24,808–24,793
cTRS-7	AUCUCGUUUAGUUCGU	28,072–28,057
GAPDH	Bio-UAUGACAACGAAUUUG	

[a] When indicated: Bio = Biotin. CS (conserved core sequence) is underlined.

Electrophoretic mobility shift assay (EMSA)

RNA–protein binding reactions were performed by incubating 10 or 1 pmol of biotinylated probe (Table 1) with 300 ng of recombinant purified protein in binding buffer (12% glycerol, 20 mM TrisHCl pH 7.4, 50 mM KCl, 1 mM EDTA, 1 mM $MgCl_2$, 1 mM DTT) 30 min at 25 °C. Reactions were loaded on a 4% non-denaturing PAGE that was run on TBE 0.5× at 150 V and 4 °C. After electrophoresis, the gel was blotted onto positively charged nylon membranes (BrightStar-Plus, Ambion) following manufacturer's instructions. Detection of the biotinylated RNA was performed using the BrightStar BioDetect kit (Ambion). When indicated, recombinant protein was previously incubated with mAb 30 min at 4 °C.

In vitro self-cleavage of RNA

Cleavage of biotin-labeled dimeric ASBVd (+) RNA was performed as previously described (Daros and Flores, 2002). Briefly, 25 ng of biotinylated RNA was incubated, under cleavage conditions, in the absence or the presence of 300 ng of recombinant protein. To minimize RNA degradation, 20 units of RNase inhibitor (SUPERase●In, Ambion) was added to the reactions. RNAs were separated by 5% denaturing PAGE. After electrophoresis, the gel was blotted and biotinylated RNAs were detected as described for the EMSA. When indicated, recombinant protein was previously incubated with 1 μl of purified mAb 30 min at 4 °C. As total RNA amount decreases with the incubation time, due to nuclease action, to estimate cleavage ratio, densitometric analysis of the 591 (uncleaved) and 247 nt (cleaved) bands was performed using Quantity One 4.5.1 Software (BioRad). In addition to be the possibly most logical reference for the cleavage reaction, it provided the same results that if other intermediate cleavage products would have been chosen for the quantification. At least three different experiments and appropriate gel exposures were used in all cases with similar results. In addition, different exposures of the same reactions were densitometered to assure that data were obtained from films within the linear range.

Annealing of RNA oligonucleotides

Biotinylated TRS-L oligonucleotide (Table 1) 0.025 μM was incubated with the same amount of unlabeled cTRS-7 oligonucleotide, in annealing buffer (40 mM TrisHCl pH 7.9,

100 mM NaCl, 20 μM EDTA, 2% glycerol). This mix was incubated 2 min at 95 °C and snap-cooled on ice. RNase inhibitor (20 U) and protein (300 ng) were added and reactions were incubated 30 min at 37 °C. Reactions were stopped by adding 1 μl of ice-cold stop solution (50 mM EDTA, 2.5% SDS, 25% glycerol, 0.01% xylene cyanol, 0.01% bromophenol blue). Samples were loaded on a 15% RNA non-denaturing PAGE with 0.1% SDS. After electrophoresis, the gel was blotted and biotinylated RNAs were detected as described for the EMSA. Densitometric analysis of the dsRNA and ssRNA bands from three different experiments was performed using Quantity One 4.5.1 Software (BioRad).

Annealing of DNA oligonucleotides

Previously described (Huang et al., 2003) oligonucleotides C and B were used. Biotinylated oligonucleotide C (0.5 nM) was incubated with unlabeled B oligonucleotide (0.4 nM), in annealing buffer (40 mM TrisHCl pH 7.9, 100 mM NaCl, 20 μM EDTA, 2% glycerol). This mix was incubated 2 min at 95 °C and snap-cooled on ice. Indicated proteins (300 ng) were added, and reactions were incubated 20 min at 37 °C. When indicated, proteinase K (150 μg/ml) was added and the reactions were incubated 10 min at 37 °C. In all cases, reactions were stopped by adding 1 μl of ice-cold stop solution (50 mM EDTA, 2.5% SDS, 25% glycerol, 0.01% xylene cyanol, 0.01% bromophenol blue). Samples were loaded on a 15% non-denaturing PAGE with 0.1% SDS. Biotinylated DNA was detected as described for the RNA annealing experiments.

In silico analysis of protein disorder

Coronavirus N proteins from several groups were analyzed using the DisProt VL3H predictor based on neural networks (Obradovic et al., 2003; Peng et al., 2005). N protein sequences used were from TGEV (GeneBank accession number AJ271965), HCoV-229E (GeneBank accession number AF304460), MHV strain A59 (GeneBank accession number AF029248), SARS-CoV Urbani strain (GeneBank accession number AJ278741), and IBV Beaudette strain (GeneBank accession number M95169).

Acknowledgments

We thank F. Almazán for critically reading the manuscript and helpful discussions. We are also grateful to J.A. Daròs, R. Flores, D.L. Black, A. Krainer, and A. Alcamí for providing plasmids and D. Dorado and M. González for technical assistance. This work was supported by grants from the Comisión Interministerial de Ciencia y Tecnología (CICYT), the Consejería de Educación y Cultura de la Comunidad de Madrid, Fort Dodge Veterinaria, and the European Communities (Frame VI, Public Health Issues Projects). SZ, IS, and JLM received fellowships from the Consejo Superior de Investigaciones Científicas (CSIC), and the European Union (QLRT-2001-00825, QLRT-2001-01050, and SP22-CT-2004-511060).

References

Airenne, K.J., Peltomaa, E., Hytönen, V.P., Laitinen, O.H., Ylä-Herttuala, S., 2003. Improved generation of recombinant baculovirus genomes in *Escherichia coli*. Nucleic Acids Res. 31 (17), e101.

Almazán, F., González, J.M., Pénzes, Z., Izeta, A., Calvo, E., Plana-Durán, J., Enjuanes, L., 2000. Engineering the largest RNA virus genome as an infectious bacterial artificial chromosome. Proc. Natl. Acad. Sci. U.S.A. 97, 5516–5521.

Almazan, F., Galan, C., Enjuanes, L., 2004. The nucleoprotein is required for efficient coronavirus genome replication. J. Virol. 78, 12683–12688.

Almazan, F., DeDiego, M.L., Galan, C., Alvarez, E., Enjuanes, L., 2006. Identification of essential genes as a strategy to select a SARS candidate vaccine using SARS-CoV infectious cDNA clone. In: Holmes, K.V., Perlman, S. (Eds.), The Nidoviruses: The Control of SARS and Other Nidovirus diseases. Kluwer Acad./Plenum Pub, NY, pp. 579–583.

Baric, R.S., Nelson, G.W., Fleming, J.O., J., D.R., Keck, J.G., Casteel, N., Stohlman, S.A., 1988. Interactions between coronavirus nucleocapsid protein and viral RNAs: implications for viral transcription. J. Virol. 62, 4280–4287.

Bertrand, E.L., Rossi, J.J., 1994. Facilitation of hammerhead ribozyme catalysis by the nucleocapsid protein of HIV-1 and the heterogeneous nuclear ribonucleoprotein A1. EMBO J. 13, 2904–2912.

Bost, A.G., Prentice, E., Denison, M.R., 2001. Mouse hepatitis virus replicase protein complexes are translocated to sites of M protein accumulation in the ERGIC at late times of infection. Virology 285, 21–29.

Brian, D.A., Spaan, W.J.M., 1997. Recombination and coronavirus defective interfering RNAs. Semin. Virol. 8, 101–111.

Calvo, E., Escors, D., Lopez, J.A., Gonzalez, J.M., Alvarez, A., Arza, E., Enjuanes, L., 2005. Phosphorylation and subcellular localization of transmissible gastroenteritis virus nucleocapsid protein in infected cells. J. Gen. Virol. 86 (8), 2255–2267.

Chang, C., Sue, S., Yu, T., Hsieh, C., Tsai, C., Chiang, Y., Lee, S., Hsiao, H., Wu, W., Chang, W., Lin, C., Huang, T., 2006. Modular organization of SARS coronavirus nucleocapsid protein. J. Biomed. Sci. 13, 59–72.

Chen, H., Gill, A., Dove, B.K., Emmett, S.R., Kemp, C.F., Ritchie, M.A., Dee, M., Hiscox, J.A., 2005. Mass spectroscopic characterization of the coronavirus infectious bronchitis virus nucleoprotein and elucidation of the role of phosphorylation in RNA binding by using surface plasmon resonance. J. Virol. 79, 1164–1179.

Choi, K.S., Huang, P., Lai, M.M., 2002. Polypyrimidine-tract-binding protein affects transcription but not translation of mouse hepatitis virus RNA. Virology 303, 58–68.

Clodi, E., Semrad, K., Schroeder, R., 1999. Assaying RNA chaperone activity in vivo using a novel RNA folding trap. EMBO J. 18, 3776–3782.

Cristofari, G., Darlix, J.L., 2002. The ubiquitous nature of RNA chaperone proteins. Prog. Nucleic Acid Res. Mol. Biol. 72, 223–268.

Cristofari, G., Ivanyi-Nagy, R., Gabus, C., Boulant, S., Lavergne, J.P., Penin, F., Darlix, J.L., 2004. The hepatitis C virus Core protein is a potent nucleic acid chaperone that directs dimerization of the viral (+) strand RNA in vitro. Nucleic Acids Res. 32, 2623–2631.

Daros, J.A., Flores, R., 2002. A chloroplast protein binds a viroid RNA in vivo and facilitates its hammerhead-mediated self-cleavage. EMBO J. 21, 749–759.

Daròs, J.A., Marcos, J.F., Hernández, C., Flores, R., 1994. Replication of avocado sunblotch viroid: evidence for a symmetric pathway with two rolling circles and hammerhead ribozyme processing. Proc. Natl. Acad. Sci. U.S.A. 91, 12813–12817.

Denison, M.R., Spaan, W.J.M., van der Meer, Y., Gibson, C.A., Sims, A.C., Prentice, E., Lu, S.T., 1999. The putative helicase of the coronavirus mouse hepatitis virus is processed from the replicase gene polyprotein and localizes in complexes that are active in viral RNA synthesis. J. Virol. 73, 6862–6871.

DeStefano, J.J., Titilope, O., 2006. Poliovirus protein 3AB displays nucleic acid chaperone and helix-destabilizing activities. J. Virol. 80, 1662–1671.

Drosten, C., Günther, S., Preiser, W., van der Werf, S., Brodt, H.-R., Becker, S., Rabenau, H., Panning, M., Kolesnikova, L., Fouchier, R.A.M., Berger, A., Burguiere, A.-M., Cinatl, J., Eickmann, M., Escriou, N., Grywna, K.,

Kramme, S., Manuguerra, J.-C., Muller, S., Rickerts, W., Sturmer, M.V.S., Klenk, H.-D., Osterhaus, A.D.M.E., 2003. Identification of a novel coronavirus in patients with severe acute respiratory syndrome. N. Engl. J. Med. 348, 1967–1976.

Enjuanes, L., Brian, D., Cavanagh, D., Holmes, K., Lai, M.M.C., Laude, H., Masters, P., Rottier, P., Siddell, S.G., Spaan, W.J.M., Taguchi, F., Talbot, P., 2000a. Coronaviridae. In: van Regenmortel, M.H.V., Fauquet, C.M., Bishop, D.H.L., Carsten, E.B., Estes, M.K., Lemon, S.M., McGeoch, D.J., Maniloff, J., Mayo, M.A., Pringle, C.R., Wickner, R.B. (Eds.), Virus Taxonomy. Classification and Nomenclature of Viruses. Academic Press, San Diego, CA, pp. 835–849.

Enjuanes, L., Spaan, W., Snijder, E., Cavanagh, D., 2000b. Nidovirales. In: van Regenmortel, M.H.V., Fauquet, C.M., Bishop, D.H.L., Carsten, E. B., Estes, M.K., Lemon, S.M., McGeoch, D.J., Maniloff, J., Mayo, M. A., Pringle, C.R., Wickner, R.B. (Eds.), Virus Taxonomy. Classification and Nomenclature of Viruses. Academic Press, San Diego, CA, pp. 827–834.

Fan, H., Ooi, A., Tan, Y.W., Wang, S., Fang, S., Liu, D.X., Lescar, J., 2005. The nucleocapsid protein of coronavirus infectious bronchitis virus: crystal structure of its N-terminal domain and multimerization properties. Structure 13, 1859–1868.

Flores, R., Daròs, J.A., Hernandez, C., 2000. The *Asunviroidae* family: viroids with hammerhead ribozymes. Adv. Virus Res. 55, 271–323.

Fouchier, R.A., Kuiken, T., Schutten, M., van Amerongen, G., van Doornum, G.J., van den Hoogen, B.G., Peiris, M., Lim, W., Stohr, K., Osterhaus, A.D., 2003. Aetiology: Koch's postulates fulfilled for SARS virus. Nature 423, 240.

González, J.M., Penzes, Z., Almazán, F., Calvo, E., Enjuanes, L., 2002. Stabilization of a full-length infectious cDNA clone of transmissible gastroenteritis coronavirus by the insertion of an intron. J. Virol. 76, 4655–4661.

Gorbalenya, A.E., Enjuanes, L., Ziebuhr, J., Snijder, E.J., 2006. Nidovirales: evolving the largest RNA virus genome. Virus Res. 117, 17–37.

He, R., Leeson, A., Andonov, A., Li, Y., Bastien, N., Cao, J., Osiowy, C., Dobie, F., Cutts, T., Ballantine, M., Li, X., 2003. Activation of AP-1 signal transduction pathway by SARS coronavirus nucleocapsid protein. Biochem. Biophys. Res. Commun. 311, 870–876.

Herschlag, D., 1995. RNA chaperones and the RNA folding problem. J. Biol. Chem. 270, 20871–20884.

Herschlag, D., Khosla, M., Tsuchihashi, Z., Karpel, R.L., 1994. An RNA chaperone activity of non-specific RNA binding proteins in hammerhead ribozyme catalysis. EMBO J. 13, 2913–2924.

Holmes, K.V., Enjuanes, L., 2003. The SARS coronavirus: a postgenomic era. Science 300, 1377–1378.

Hong, M.K., Harbron, E.J., O'Connor, D.B., Guo, J., Barbara, P.F., Levin, J.G., Musier-Forsyth, K., 2003. Nucleic acid conformational changes essential for HIV-I nucleocapsid protein-mediated inhibition of self-priming in minus-strand transfer. J. Mol. Biol. 325, 1–10.

Huang, P., Lai, M.M.C., 2001. Heterogeneous nuclear ribonucleoprotein A1 binds to the 3′-untranslated region and mediates potential 5′–3′-end cross talks of mouse hepatitis virus RNA. J. Virol. 75, 5009–5017.

Huang, Z.S., Wu, H.N., 1998. Identification and characterization of the RNA chaperone activity of hepatitis delta antigen peptides. J. Biol. Chem. 273, 26455–26461.

Huang, Z.S., Su, W.H., Wang, J.L., Wu, H.N., 2003. Selective strand annealing and selective strand exchange promoted by the N-terminal domain of hepatitis delta antigen. J. Biol. Chem. 278, 5685–5693.

Huang, Q., Yu, L., Petros, A.M., Gunasekera, A., Liu, Z., Xu, N., Hajduk, P., Mack, J., W., F.S., Olejniczak, E.T., 2004. Structure of the N-terminal RNA-binding domain of the SARS CoV nucleocapsid protein. Biochemistry 20, 6059–6063.

Hurst, K.R., Kuo, L., Koetzner, C.A., Ye, R., Hsue, B., Masters, P.S., 2005. A major determinant for membrane protein interaction localizes to the carboxy-terminal domain of the mouse coronavirus nucleocapsid protein. J. Virol. 79, 13285–13297.

Iakoucheva, L.M., Brown, C.J., Lawson, J.D., Obradovic, Z., Dunker, A.K., 2002. Intrinsic disorder in cell-signaling and cancer-associated proteins. J. Mol. Biol. 323, 573–584.

Ivanyi-Nagy, R., Davidovic, L., Khandjian, E.W., Darlix, J.L., 2005. Disordered RNA chaperone proteins: from functions to disease. Cell. Mol. Life. Sci. 62 (13), 1409–1417.

Ksiazek, T.G., Erdman, D., Goldsmith, C., Zaki, S., Peret, T., Emery, S., Tong, S., Urbani, C., Comer, J.A., Lim, W., Rollin, P.E., Dowell, S., Ling, A.-E., Humphrey, C., Shieh, W.-J., Guarner, J., Paddock, C.D., Rota, P., Fields, B., DeRisi, J., Yang, J.-Y., Cox, N., Hughes, J., LeDuc, J.W., Bellini, W.J., Anderson, L.J., 2003. A novel coronavirus associated with severe acute respiratory syndrome. N. Engl. J. Med. 348, 1953–1966.

Kuiken, T., Fouchier, R.A.M., Schutten, M., Rimmelzwaan, G.F., van Amerongen, G., van Riel, D., Laman, J.D., de Jong, T., van Doornum, G., Lim, W., Ling, A.E., Chan, P.K.S., Tam, J.S., Zambon, M.C., Gopal, R., Drosten, C., van der Werf, S., Escriou, N., Manuguerra, J.-C., Stohr, K., Peiris, J.S.M., 2003. Newly discovered coronavirus as the primary cause of severe acute respiratory syndrome. Lancet 362, 263–270.

Laude, H., Masters, P.S., 1995. The coronavirus nucleocapsid protein. In: Siddell, S.G. (Ed.), The Coronaviridae. Plenum Press, New York, pp. 141–158.

Levin, J.G., Guo, J., Rouzina, I., Musier-Forsyth, K., 2005. Nucleic acid chaperone activity of HIV-1 nucleocapsid protein: critical role in reverse transcription and molecular mechanism. Prog. Nucleic Acid Res. Mol. Biol. 80, 217–286.

Lorsch, J.R., 2002. RNA chaperones exist and DEAD box proteins get a life. Cell 109, 797–800.

Marra, M.A., Jones, S.J.M., Astell, C.R., Holt, R.A., Brooks-Wilson, A., Butterfield, Y.S.N., Khattra, J., Asano, J.K., Barber, S.A., Chan, S.Y., Cloutier, A., Coughlin, S.M., Freeman, D., Girn, N., Griffith, O.L., Leach, S.R., Mayo, M., McDonald, H., Montgomery, S.B., Pandoh, P.K., Petrescu, A.S., Robertson, A.G., Schein, J.E., Siddiqui, A., Smailus, D.E., Stott, J.M., Yang, G.S., Plummer, F., Andonov, A., Artsob, H., Bastien, N., Bernard, K., Booth, T.F., Bowness, D., Czub, M., Drebot, M., Fernando, L., Flick, R., Garbutt, M., Gray, M., Grolla, A., Jones, S., Feldmann, H., Meyers, A., Kabani, A., Li, Y., Normand, S., Stroher, U., Tipples, G.A., Tyler, S., Vogrig, R., Ward, D., Watson, B., Brunham, R.C., Krajden, M., Petric, M., Skowronski, D.M., Upton, C., Roper, R.L., 2003. The genome sequence of the SARS-associated coronavirus. Science 300, 1399–1404.

Martín-Alonso, J.M., Balbín, M., Garwes, D.J., Enjuanes, L., Gascón, S., Parra, F., 1992. Antigenic structure of transmissible gastroenteritis virus nucleoprotein. Virology 188, 168–174.

Mir, M.A., Panganiban, A.T., 2005. The hantavirus nucleocapsid protein recognizes specific features of the viral RNA panhandle and is altered in conformation upon RNA binding. J. Virol. 79, 1824–1835.

Mir, M.A., Panganiban, A.T., 2006. Characterization of the RNA chaperone activity of hantavirus nucleocapsid protein. J. Virol. 80 (13), 6276–6285.

Mohr, S., Stryker, J.M., Lambowitz, A.M., 2002. A DEAD-box protein functions as an ATP-dependent RNA chaperone in group I intron splicing. Cell 109 (6), 769–779.

Nagy, P.D., Simon, A.E., 1997. New insights into the mechanisms of RNA recombination. Virology 235, 1–9.

Nelson, G.W., Stohlman, S.A., Tahara, S.M., 2000. High affinity interaction between nucleocapsid protein and leader/intergenic sequence of mouse hepatitis virus RNA. J. Gen. Virol. 81, 181–188.

Obradovic, Z., Peng, K., Vuceti, S., Radivojac, P., Brown, C., Dunker, A.K., 2003. Predicting intrinsic disorder from aminoacid sequence. Proteins 53, 566–572.

Parker, M.M., Masters, P.S., 1990. Sequence comparison of the N genes of five strains of the coronavirus mouse hepatitis virus suggests a three domain structure for the nucleocapsid protein. Virology 179, 463–468.

Pasternak, A.O., van den Born, E., Spaan, W.J.M., Snijder, E.J., 2001. Sequence requirements for RNA strand transfer during nidovirus discontinuous subgenomic RNA synthesis. EMBO J. 20, 7220–7228.

Pasternak, A.O., van den Born, E., Spaan, W.J.M., Snijder, E.J., 2003. The stability of the duplex between sense and antisense transcription-regulating sequences is a crucial factor in arterivirus subgenomic mRNA synthesis. J. Virol. 77, 1175–1183.

Pasternak, A.O., Spaan, W.J., Snijder, E.J., 2006. Nidovirus transcription: how to make sense? J. Gen. Virol. 87, 1403–1421.

Peng, K., Vuceti, S., Radivojac, P., Brown, C.J., Dunker, A.K., Obradovic, Z.,

2005. Optimizing intrinsic disorder predictors with protein evolutionary information. J. Bioinfo. Comput. Biol. 3 (1), 35–60.

Pontius, B.W., Berg, P., 1992. Rapid assembly and disassembly of complementary DNA strands through as equilibrium. J. Biol. Chem. 267, 13815–13818.

Portman, D.S., Dreyfuss, G., 1994. RNA annealing activities in HeLa nuclei. EMBO J. 13, 213–221.

Rajkowitsch, L., Semrad, K., Mayer, O., Schroeder, R., 2005. Assays for the RNA chaperone activity of proteins. Biochem. Soc. Trans. 33, 450–456.

Risco, C., Antón, I.M., Enjuanes, L., Carrascosa, J.L., 1996. The transmissible gastroenteritis coronavirus contains a spherical core shell consisting of M and N proteins. J. Virol. 70, 4773–4777.

Romero, P., Obradovic, Z., Dunker, A.K., 1997. Identifying disordered regions in proteins from aminoacid sequences. Proc. IEEE Int. Conf. Neural Networks 1, 90–95.

Rota, P.A., Oberste, M.S., Monroe, S.S., Nix, W.A., Campganoli, R., Icenogle, J.P., Peñaranda, S., Bankamp, B., Maher, K., Chen, M.-H., Tong, S., Tamin, A., Lowe, L., Frace, M., DeRisi, J.L., Chen, Q., Wang, D., Erdman, D.d., Peret, T.C.T., Burns, C., Ksiazek, T.G., Rollin, P.E., Sanchez, A., Liffick, S., Holloway, B., Limor, J., McCaustland, K., Olsen-Rassmussen, M., Fouchier, R., Gunther, S., Osterhaus, A.D.M.E., Drosten, C., Pallansch, M.A., Anderson, L.J., Bellini, W.J., 2003. Characterization of a novel coronavirus associated with severe acute respiratory syndrome. Science 300, 1394–1399.

Sawicki, S.G., Sawicki, D.L., 1998. A new model for coronavirus transcription. Adv. Exp. Med. Biol. 440, 215–220.

Schelle, B., Karl, N., Ludewig, B., Siddell, S.G., Thiel, V., 2005. Selective replication of coronavirus genomes that express nucleocapsid protein. J. Virol. 79, 6620–6630.

Schroeder, R., Barta, A., Semrad, K., 2004. Strategies for RNA folding and assembly. Nat. Rev., Mol. Cell Biol. 5, 908–919.

Shi, S.T., Huang, P., Li, H.P., Lai, M.M.C., 2000. Heterogeneous nuclear ribonucleoprotein A1 regulates RNA synthesis of a cytoplasmic virus. EMBO J. 19, 4701–4711.

Sola, I., Moreno, J.L., Zuñiga, S., Alonso, S., Enjuanes, L., 2005. Role of nucleotides immediately flanking the transcription-regulating sequence core in coronavirus subgenomic mRNA synthesis. J. Virol. 79, 2506–2516.

St-Jean, J.R., Desforges, M., Almazan, F., Jacomy, H., Enjuanes, L., Talbot, P.J., 2006. Recovery of a neurovirulent human coronavirus OC43 from an infectious cDNA clone. J. Virol. 80 (7), 3670–3674.

Stohlman, S.A., Baric, R.S., Nelson, G.N., Soe, L.H., Welter, L.M., Deans, R.J., 1988. Specific interaction between coronavirus leader RNA and nucleocapsid protein. J. Virol. 62, 4288–4295.

Surjit, M., Liu, B., Jameel, S., Chow, V.T., Lal, S.K., 2004. The SARS coronavirus nucleocapsid protein induces actin reorganization and apoptosis in COS-1 cells in the absence of growth factors. Biochem. J. 383, 13–18.

Thiel, V., Herold, J., Schelle, B., Siddell, S., 2001. Infectious RNA transcribed in vitro from a cDNA copy of the human coronavirus genome cloned in vaccinia virus. J. Gen. Virol. 82, 1273–1281.

Tompa, P., Csermely, P., 2004. The role of structural disorder in the function of RNA and protein chaperones. FASEB J. 18, 1169–1175.

Tsuchihashi, Z., Brown, P.O., 1994. DNA strand exchange and selective DNA annealing promoted by the Human Immunodeficiency Virus Type I nucleocapsid protein. J. Virol. 68, 5863–5870.

van der Hoek, L., Pyrc, K., Jebbink, M.F., Vermeulen-Oost, W., Berkhout, R.J., Wolthers, K.C., Wertheim-van Dillen, P.M., Kaandorp, J., Spaargaren, J., Berkhout, B., 2004. Identification of a new human coronavirus. Nat. Med. 10, 368–373.

Wang, C.C., Chang, T.C., Lin, C.W., Tsui, H.L., Chu, P.B., Chen, B.S., Huang, Z.S., Wu, H.N., 2003. Nucleic acid binding properties of the nucleic acid chaperone domain of hepatitis delta antigen. Nucleic Acids Res. 31, 6481–6492.

Woo, P.C., Lau, S.K., Chu, C.M., Chan, K.H., Tsoi, H.W., Huang, Y., Wong, B.H., Poon, R.W., Cai, J.J., Luk, W.K., Poon, L.L., Wong, S.S., Guan, Y., Peiris, J.S., Yuen, K.Y., 2005. Characterization and complete genome sequence of a novel coronavirus, coronavirus HKU1, from patients with pneumonia. J. Virol. 79, 884–895.

Xie, J., Lee, J., Kress, T.L., Mowry, K.L., Black, D.L., 2003. Protein kinase A phosphorylation modulates transport of the polypyrimidine tract-binding protein. Proc. Natl. Acad. Sci. U.S.A. 100 (15), 8776–8781.

Youn, S., Leibowitz, J., Collisson, E.W., 2005. In vitro assembled, recombinant infectious bronchitis viruses demonstrate that the 5a open reading frame is not essential for replication. Virology 332 (1), 206–215.

Yount, B., Curtis, K.M., Baric, R.S., 2000. Strategy for systematic assembly of large RNA and DNA genomes: the transmissible gastroenteritis virus model. J. Virol. 74, 10600–10611.

Yount, B., Curtis, K.M., Fritz, E.A., Hensley, L.E., Jahrling, P.B., Prentice, E., Denison, M.R., Geisbert, T.W., Baric, R.S., 2003. Reverse genetics with a full-length infectious cDNA of severe acute respiratory syndrome coronavirus. Proc. Natl. Acad. Sci. U.S.A. 100, 12995–13000.

Yu, I., Gustafson, C.L.T., Diao, J., W., B.J., Li, Z., Zhang, J., Chen, J., 2005. Recombinant severe acute respiratory syndrome (SARS) coronavirus nucleocapsid protein forms a dimer through its C-terminal domain. J. Biol. Chem. 280, 23280–23286.

Zuñiga, S., Sola, I., Alonso, S., Enjuanes, L., 2004. Sequence motifs involved in the regulation of discontinuous coronavirus subgenomic RNA synthesis. J. Virol. 78, 980–994.